Multicriticality in the Blume–Capel model under a continuous-field probability distribution

2010 J. Phys. A: Math. Theor. 43 125003

(http://iopscience.iop.org/1751-8121/43/12/125003)

IOP PUBLISHING JOURNAL OF PHYSICS A: MATHEMATICAL AND THEORETICAL

J. Phys. A: Math. Theor. **43** (2010) 125003 (10pp) doi:10.1088/1751-8113/43/12/125003

Multicriticality in the Blume–Capel model under a continuous-field probability distribution

Octavio D Rodriguez Salmon[1] **and Justo Rojas Tapia**[2]

[1] Centro Brasileiro de Pesquisas Físicas and National Institute of Science and Technology for Complex Systems, Rua Xavier Sigaud 150 22290-180 Rio de Janeiro, Brazil
[2] Universidad Nacional Mayor de San Marcos, Facultad de Ciencias Físicas, Av. Venezuela s/n, Apartado Postal 14-0149, Lima-1, Peru

E-mail: octavior@cbpf.br and jrojast@unmsm.edu.pe

Received 16 October 2009, in final form 27 January 2010
Published 5 March 2010
Online at stacks.iop.org/JPhysA/43/125003

Abstract

The multicritical behavior of the Blume–Capel model with infinite-range interactions is investigated by introducing quenched disorder in the crystal field Δ_i, which is represented by a superposition of two Gaussian distributions with the same width σ, centered at $\Delta_i = \Delta$ and $\Delta_i = 0$, with probabilities p and $(1 - p)$, respectively. A rich variety of phase diagrams is presented, and their distinct topologies are shown for different values of σ and p. The tricritical behavior is analyzed through the existence of fourth-order critical points, as well as how the complexity of the phase diagrams is reduced by the strength of the disorder.

PACS numbers: 05.50.+q, 64.60.De, 75.10.Hk, 75.40.Cx

1. Introduction

The effect of disorder on different types of condensed matter orderings is nowadays a subject of considerable interest [1, 2]. For the case of disordered magnetic systems, random-field spin models have been systematically studied, not only for theoretical interests but also for some identifications with experimental realizations [3]. An interesting issue is the study of how quenched randomness destroys some types of criticalities. So, in what concerns the effect produced by random fields in low dimensions, it has been noticed [4, 5] that first-order transitions will be replaced by continuous transitions, so tricritical points and critical end points will be depressed in temperature, and a finite amount of disorder will suppress them. Nevertheless, in two dimensions, an infinitesimal amount of field randomness seems to destroy any first-order transition [6, 7]. Interestingly, the simplest model exhibiting a tricritical phase diagram in the absence of randomness is the Blume–Capel model. The Blume–Capel model [8, 9] is a regular Ising model for spin-1 used to model ^{4}He–^{3}He mixtures [10]. The interesting

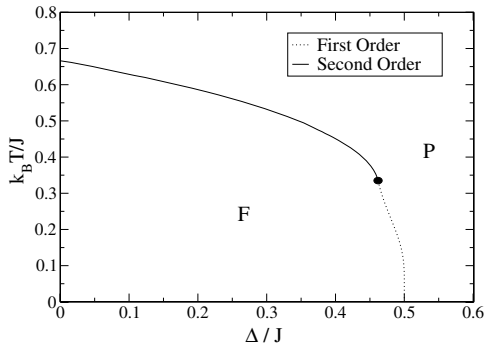

Figure 1. Phase diagram of the Blume–Capel model in the plane $k_B T/J - \Delta/J$ within the mean-field approach, where k_B is the Boltzman constant, T is the temperature, $J > 0$ is the coupling constant between each pair of spins and Δ is the crystal field (also called the anisotropy field), which is regarded constant (without disorder) for each site i. The black circle represents the tricritical point. The ferromagnetic and paramagnetic phases are represented by **F** and **P**, respectively. The full line represents the continuous or second-order critical frontier, and the dotted line is for the first-order frontier.

feature is the existence of a tricritical point in the phase diagram represented in the plane of temperature versus crystal field, as shown in figure 1. This phase diagram was firstly obtained in the mean-field approach, but the same qualitative properties were also observed in low dimensions. The latter was confirmed through some approximation techniques as well as by Monte Carlo simulations [11–15]. Also, the tricritical behavior is still held in two dimensions [16–19]. Nevertheless, in other models this situation is controversial. For example, the random-field Ising model in the mean-field approach [20] also exhibits a tricritical point, but some Monte Carlo simulations [21] in the cubic lattice suggest that this is only an artifact of the mean-field calculations. Accordingly, this interesting fact in the Blume–Capel model motivated some authors to explore the richness of this model, within the mean-field approach, by introducing disorder in the crystal field [22–25] as well as by adding an external random field [26]. For the former case, a variety of phase diagrams including different critical points with some similar topologies found for the random-field spin-1/2 Ising model [27, 28] were obtained. However, in those studies, the fourth-order critical points, which limit the existence of tricritical points, were overlooked. Consequently, our aim in this work is to improve those previous studies by considering a more general probability distribution function for the crystal field and bettering some results given in [23–25]. The next section is dedicated to define the model and the special critical points produced by it.

2. The model

The infinite-range-interaction Blume–Capel model is given by the following Hamiltonian:

$$\mathcal{H} = -\frac{J}{N}\sum_{(i,j)} S_i S_j + \sum_i \Delta_i S_i^2, \tag{1}$$

where $S_i = -1, 0, 1$ and N is the number of spins. The first sum runs over all distinct pairs of spins. The coupling constant J is divided by N in order to maintain the extensivity. The

crystal fields are represented by quenched variables $\{\Delta_i\}$, obeying the probability distribution function (PDF) given by

$$P(\Delta_i) = \frac{p}{\sqrt{2\pi}\,\sigma}\exp\left[-\frac{(\Delta_i-\Delta)^2}{2\sigma^2}\right] + \frac{(1-p)}{\sqrt{2\pi}\,\sigma}\exp\left[-\frac{{\Delta_i}^2}{2\sigma^2}\right], \tag{2}$$

which consists of a superposition of two independent Gaussian distributions with the same width σ, centered at $\Delta_i = \Delta$ and $\Delta_i = 0$, with probabilities p and $(1-p)$, respectively. For $\sigma = 0$, we recover the bimodal distribution studied in [23, 24], and for $p = 1$, the simple Gaussian one of reference [25] . For $\sigma = 0$ and $p = 1$, we return to the simple Blume–Capel model without randomness [10].

By standard procedures [28], we obtain the analytical expression for the free energy per spin (f), through which a self-consistent equation for the magnetization m may be obtained. Thus, we have the following relations at the equilibrium:

$$f = \frac{1}{2}Jm^2 - \frac{1}{\beta}E\left\{\log(2\exp(-\beta\Delta_i)\cosh(\beta Jm)+1)\right\}, \tag{3}$$

$$m = \sinh(\beta m)E\left\{\left[\cosh(\beta m) + \tfrac{1}{2}\exp(\beta\Delta_i)\right]^{-1}\right\}, \tag{4}$$

where the quenched average, represented by $E\{\cdots\}$, is taken with respect to the PDF given in equation (2), and $\beta = 1/(k_BT)$. To write conditions for locating tricritical and fourth-order critical points, we expand the right-hand side of equation (4) in powers of m (Landau's expansion, see [29]). Conveniently, we expand the magnetization up to seventh order in m, so

$$m = A_1m + A_3m^3 + A_5m^5 + A_7m^7 + \cdots, \tag{5}$$

where

$$A_1 = \beta E\{g_i\}, \tag{6}$$

$$A_3 = \beta^3 E\left\{\left(\tfrac{1}{6}g_i - \tfrac{1}{2}g_i^2\right)\right\}, \tag{7}$$

$$A_5 = \beta^5 E\left\{\left(\tfrac{1}{120}g_i - \tfrac{1}{8}g_i^2 + \tfrac{1}{4}g_i^3\right)\right\}, \tag{8}$$

$$A_7 = \beta^7 E\left\{\left(\tfrac{1}{5040}g_i - \tfrac{1}{80}g_i^2 + \tfrac{1}{12}g_i^3 - \tfrac{1}{8}g_i^4\right)\right\} \tag{9}$$

and

$$g_i = \left(1 + \tfrac{1}{2}\exp(\beta\Delta_i)\right)^{-1}. \tag{10}$$

In order to obtain the continuous critical frontier, one sets $A_1 = 1$, provided that $A_3 < 0$. If a first-order critical frontier begins after the continuous one, the latter line ends at a tricritical point if $A_3 = 0$, provided that $A_5 < 0$. The possibility of a fourth-order critical point is given for $A_1 = 1$, $A_3 = 0$, $A_5 = 0$ and $A_7 < 0$. Thus, a fourth-order point may be regarded as the last tricritical point.

By taking $\beta \to \infty$ ($T \to 0$), we obtain the asymptotic limit of equations (3) and (4), so we have

$$\begin{aligned} f = {} & \frac{1}{2}Jm^2 - p\left(\frac{1}{2}(Jm-\Delta)\left(1+\operatorname{erf}\left[\frac{Jm-\Delta}{\sqrt{2}\,\sigma}\right]\right) + \frac{\sigma}{\sqrt{2\pi}}\exp\left[-\frac{(Jm-\Delta)^2}{2\,\sigma^2}\right]\right) \\ & - (1-p)\left(\frac{1}{2}Jm\left(1+\operatorname{erf}\left[\frac{Jm}{\sqrt{2}\sigma}\right]\right) + \frac{\sigma}{\sqrt{2\pi}}\exp\left[-\frac{J^2m^2}{2\sigma^2}\right]\right), \end{aligned} \tag{11}$$

$$m = \frac{p}{2}\left(1+\operatorname{erf}\left[\frac{Jm-\Delta}{\sqrt{2}\,\sigma}\right]\right) + \frac{(1-p)}{2}\left(1+\operatorname{erf}\left[\frac{Jm}{\sqrt{2}\,\sigma}\right]\right), \tag{12}$$

where

$$\operatorname{erf}\left(\frac{x}{\sqrt{2}}\right) = \sqrt{\frac{2}{\pi}} \int_0^x \mathrm{d}z \mathrm{e}^{-z^2/2}. \tag{13}$$

The critical frontiers, for a given pair (σ, p), are obtained by solving a nonlinear set of equations, which consist of equating the free energies for the corresponding phases (Maxwell's construction), and the respective magnetization equations based on the relations given in equations (3) and (4). We must carefully verify that every numerical solution minimizes the free energy.

The symbols used to represent the different critical lines and points [28] are as follows:

- continuous or second-order critical frontier: continuous line;
- first-order critical frontier: dotted line;
- tricritical point: located by a black circle;
- fourth-order critical point: located by an empty square;
- ordered critical point: located by an asterisk;
- critical end point: located by a black triangle.

To clarify, a continuous critical frontier is that which separates two distinct phases through which the order parameter changes continuously pass from one phase to another. This is contrary to the case of the first-order transition through which, the order parameter suffers a discontinuous change, so the two corresponding phases coexist as each critical point. A tricritical point is basically the point in which a continuous line terminates to give rise a first-order critical line. A fourth-order critical point is sometimes called a vestigial tricritical point, because it may be regarded as the last tricritical point. An ordered critical point is the point, inside an ordered region, where a first-order critical line ends, above which the order parameter passes smoothly from one ordered phase to the other. Finally, a critical end point corresponds to the intersection of a continuous line that separates the paramagnetic from one of the ferromagnetic phases with a first-order line separating the paramagnetic and the other ferromagnetic phase. In the following section, we make use of these definitions.

3. Results and discussion

The distinct phase diagrams for the present model were numerically obtained by scanning the whole p-domain for each σ-width. So distinct topologies belonging to different p-ranges were found for a given σ. For instance, figure 2 shows the whole variety of them for a small $\sigma/J = 0.1$, for each arbitrary representative p.

Note that for small values of p, only one ferromagnetic order appears at low temperatures, as shown in figure 2(a) for $p = 0.15$. We designate it as topology I. Figures 2(b) and (c) ($p = 0.5, 0.8$) represent the same topology (topology II), which consists of one first-order critical line separating two different ferromagnetic phases $\mathbf{F_1}$ and $\mathbf{F_2}$, and a continuous line remaining for $\Delta/J \to \infty$. Figure 2(c), though qualitatively the same as in figure 2(b), is intended to show how the first-order line and the continuous line approach themselves as p increases. Figure 2(d) shows topology III, for $p = 0.85$, so the preceding first-order line is now dividing the continuous line by two critical end points. Note that the upper continuous line terminates, following a re-entrant path, at a critical end point where the phases $\mathbf{F_1}$, $\mathbf{F_3}$ and $\mathbf{P}$ coexist. So, at the lower critical end point, $\mathbf{F_1}$, $\mathbf{F_2}$ and $\mathbf{P}$ coexist. Above the ordered critical point, the order parameter passes smoothly from $\mathbf{F_1}$ to $\mathbf{F_3}$ (see the inset there). If we increase p up to some $p = p^*$, the upper continuous line and the first-order line will be met at a fourth-order point (represented by a square) as shown in figure 2(e). Thus, p^* is the threshold

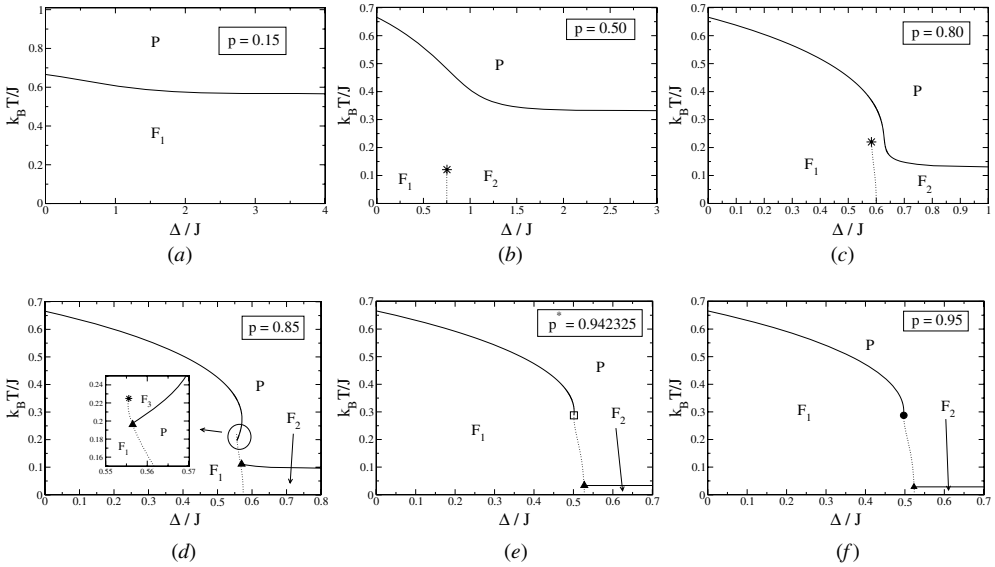

Figure 2. Phase diagrams of the Blume–Capel model whose crystal field obeys the PDF given in equation (2). For $\sigma/J = 0.1$, the diagrams show a variety of topologies according to the probability p. For convenience, we classify them into four topologies, so in (a) topology I is shown; in (b) and (c) topology II; in (d) topology III, and then in (e) and (f) topology IV. The symbols representing special critical points are interpreted in the text.

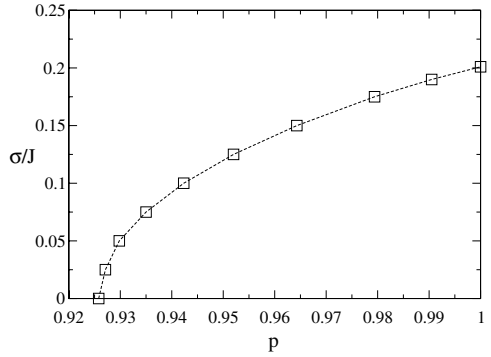

Figure 3. Some fourth-order critical points located in the plane p–σ/J. Note that if $\sigma = 0$, we recover the bimodal case studied in [23, 24], where we found $p^* = 0.9258$, just in agreement with them. Note that if $p = 1$, $\sigma/J = 0.202$, then it is a σ-limit for the tricritical behavior. The dashed line is only a guide.

for topology IV. Then, for $p > p^*$, those lines will be met at a tricritical point, as noticed in figure 2(f). Conversely, tricritical points appear for $p > p^*$, so the last one for $p = p^*$. The same types of phase diagrams are found in [23–25]. Nevertheless, we improve their results, not only bettering some of their numerical calculations but also in that we may now locate the regions of validity of these topologies in the plane σ/J–p. To this end, we start by locating the fourth-order points in the plane σ/J–p, as shown in figure 3.

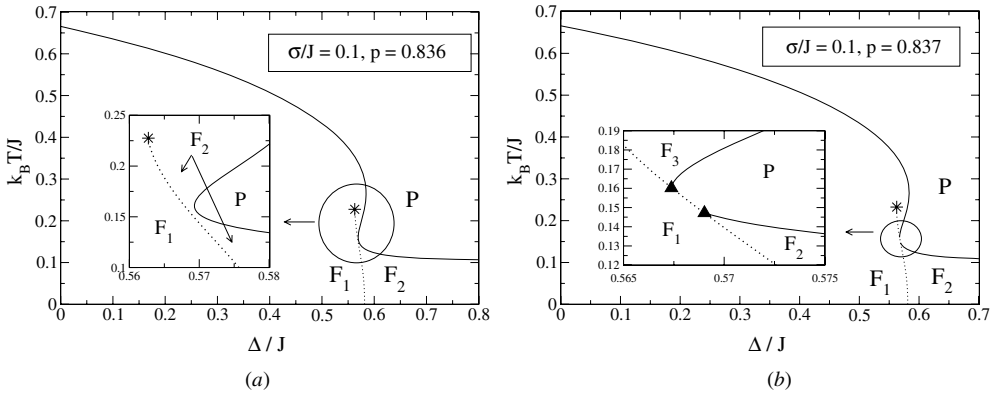

Figure 4. Phase diagrams (for $\sigma/J = 0.1$) showing two slightly different values of p, between which there is a critical p for passing from topology II to III. So, that critical point must be found for $p = 0.8365 \pm 0.0005$.

Note that $\sigma/J = 0.202$ is a cut-off for the tricritical behavior. Then, topology IV will no longer be found for greater widths. On the other hand, we determine the threshold for topology III, by estimating numerically which value of p, for each σ/J, produces a situation like that presented in figure 4 (case $\sigma/J = 0.1$), where we see how topology III emerges for a p slightly greater than 0.836. For the special case $\sigma/J = 0$, we found this threshold for $p = 0.8245$, which was not calculated in [24]. However, it is worthwhile to mention that in [23] (case $\sigma/J = 0$), the authors ignored the existence of the second ferromagnetic phase $\mathbf{F_2}$ appearing at low temperatures and large Δ/J in topology III, so a greater value of p ($p < 8/9 = 0.888\ldots$) was found by them as an inferior limit of this topology. This error was noticed by the authors in [24], but they did not give any limit value for this threshold as we have already mentioned. For completeness, figure 5 illustrates that this type of phase diagram (topology III) is still present even for a smaller p ($p < 8/9$), as confirmed by the free energy evaluated at three distinct $(k_BT/J, \Delta/J)$-points along the first-order critical line, at which there are three types of coexistences, namely, $\mathbf{F_1}$ with $\mathbf{F_3}$, $\mathbf{F_1}$ with $\mathbf{P}$, and $\mathbf{F_1}$ with $\mathbf{F_2}$. On the other hand, we also noted another discrepancy with respect to a critical σ/J, found in [25], above which topology III disappears for $p = 1$. There, the authors affirmed that if $\sigma/J > 0.229$, the paramagnetic–ferromagnetic transition becomes second order at all temperatures, but we noticed (and checked it by plotting the free energy) that it only happens for a greater width, namely $\sigma/J = 0.283$. We think that the reason of this difference may be on account of having better computation power now.

In order to obtain the frontier which separates topologies I and II (in the plane σ/J–p), we have to find the corresponding p, for a given σ/J, that locates the ordered critical point at $T = 0$. To this end, we focus the rest of this section on zero-temperature calculations.

In order to perform zero temperature calculations, we make use of equations (11) and (12). Consequently, for $\sigma/J = 0$ (see reference [24]), there are two ferromagnetic phases $\mathbf{F_1}$ and $\mathbf{F_2}$ coexisting at $\Delta/J = 1 - p/2$, having magnetizations $m_1 = 1$ and $m_2 = 1 - p$, respectively. We observed that these relations still remain up to some finite σ, after which a σ-dependence emerges. So, for a greater width called σ', the ordered critical point (that of topology III) must be found at $T = 0$. Then, the first-order critical line is suppressed and only one ferromagnetic order exists for any p. For instance, if we choose $p = 0.5$, we find $\sigma'/J = 0.2$, as illustrated in figure 6. There, the zero temperature free energy versus the order parameter is plotted for

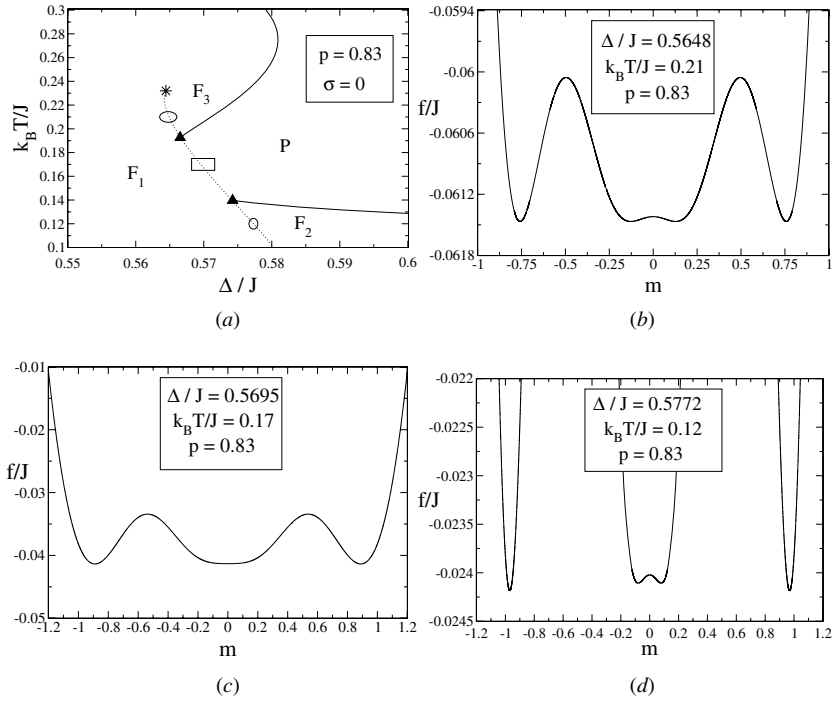

Figure 5. In (*a*) the most critical region of the phase diagram for $\sigma = 0$ is shown, and $p = 0.83$. It is a typical phase diagram for topology III (like that of figure 2(*d*)). Note that three points belonging to the first-order critical line are highlighted by an ellipse, a rectangle and a circle. The ellipse is surrounding a critical point where the phases $\mathbf{F_1}$ and $\mathbf{F_3}$ coexist, as confirmed through the free energy versus the magnetization in (*b*). In (*c*) and (*d*), the free energy shows which phases are coexisting at the points surrounded by the rectangle and the circle. Thus, in (*c*), the phases $\mathbf{F_1}$ and $\mathbf{P}$ coexist, because two symmetric minima at finite values of m, and one minimum at $m = 0$, are at the same level. In (*d*), like in (*b*), four symmetric minima at the same level are shown. Therefore, phases $\mathbf{F_1}$ and $\mathbf{F_2}$ coexist at this critical point.

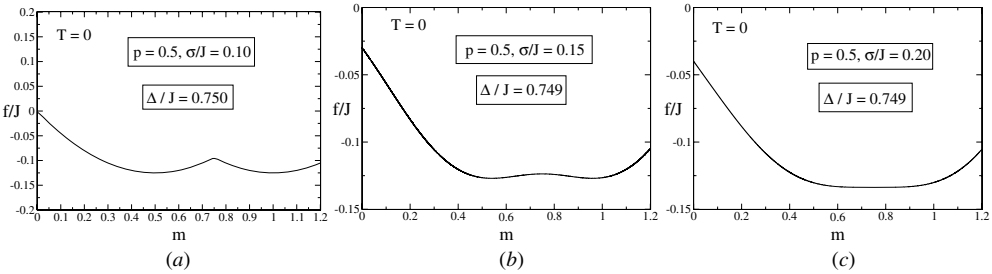

Figure 6. The free energy (see equation (11)) versus the order parameter, plotted for $p = 0.5$, for three different values of σ/J. In (*a*) and (*b*), two ferromagnetic phases coexist but in (*c*) we note that for $\sigma/J = 0.2$, there is already a crossover to pass from one ferromagnetic phase to the other.

three different values of σ/J, at the point where $\mathbf{F_1}$ and $\mathbf{F_2}$ coexist. Thus, in (*a*), two minima are at the same level for $\sigma = 0.1$. In (*b*), it still happens for $\sigma = 0.15$. Nonetheless, in (*c*), for $\sigma/J = 0.2$, the ordered critical point is already at $T = 0$. Therefore, for this particular p, there is only a ferromagnetic phase for $\sigma/J > 0.2$.

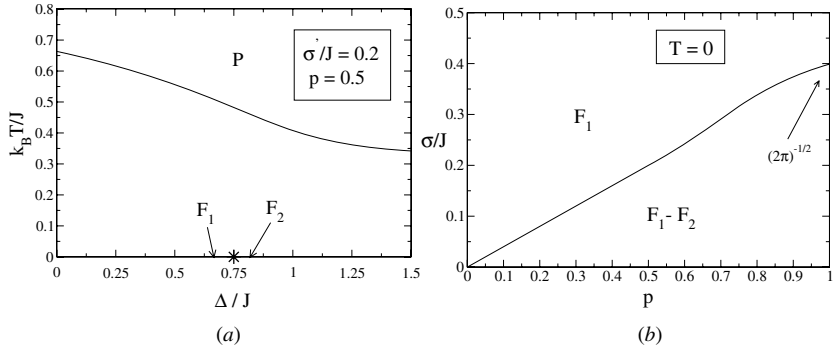

Figure 7. In (*a*) the phase diagram obtained for $p = 0.5$ is shown, for the corresponding critical σ'/J. Note that the ordered-critical point (that appeared in topology II) is now located at the horizontal axis. So, for $\sigma > \sigma'$ there will be only one ferromagnetic order at low temperatures for $p = 0.5$. In (*b*), the line separates topologies I and II. This line is made of points numerically obtained by finding σ'/J, for each p.

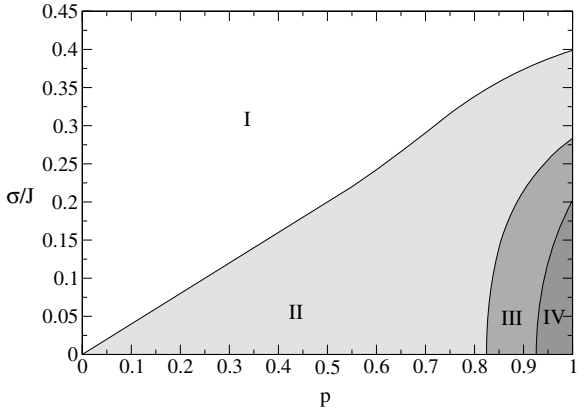

Figure 8. Regions, in the plane σ/J versus p, associated with the topologies for the present model (see also figure 2). The horizontal and the vertical axes represent the probability p and the width σ, respectively (see equation (2)). The tricritical behavior belongs to the region IV. The simplest topology belongs to region I, where only one ferromagnetic phase appears, whereas the rest topologies contain two ferromagnetic orders at low temperatures.

For completeness, figure 7(*a*) shows what figure 6(*c*) illustrates by means of the free energy. There, it is shown where the ordered critical point is located at $T = 0$. In figure 7(*b*), we see the line composed by the $(p, \sigma'/J)$-points. This line separates phase diagrams containing two and one ferromagnetic phases. Particularly, for $p = 1$, $\sigma'/J = (2\pi)^{-1/2}$, as obtained in [25] and confirmed numerically by us. We summarize the preceding analysis by showing, in figure 8, the regions of validity for the four qualitatively distinct phase diagrams. Note that along the horizontal axis ($\sigma/J = 0$), regions II and III are separated by $p = 0.8245$ and regions III and IV by $p = 0.9258$. Along the vertical axis (at $p = 1$), regions IV and III are separated by $\sigma/J = 0.202$, regions III and II by $\sigma/J = 0.283$, and then regions II and I by $\sigma/J = (2\pi)^{-1/2} \approx 0.3989$. Furthermore, the line separating topologies I and II is the same as in figure 7(*b*). The frontier separating topologies II and III consists of points estimated by

the analysis illustrated by figure 4. Finally, the line between topologies III and IV is made of fourth-order critical points, i.e. it is based upon the points in figure 3.

4. Conclusions

We revisit the study of the infinite-range-interaction spin-1 Blume–Capel model with quenched randomness, by considering a more general probability distribution function for the crystal field Δ_i, which consists of two Gaussian distributions centered at $\Delta_i = \Delta$ and $\Delta_i = 0$, with probabilities p and $(1 - p)$, respectively. For $\sigma = 0$, we recover the bimodal case studied in [23, 24], and for $p = 1$, the Gaussian case studied in [25]. For σ-widths in $0 < \sigma < 0.202J$, the system exhibits four distinct topologies according to the range in which p belongs. So, we designate them as topologies I, II, III and IV, in increasing order of p. Topology I contains one continuous critical line separating a ferromagnetic phase from the paramagnetic phase. In topology II, one first-order critical line separating two ferromagnetic phases is added. This line terminates at an ordered critical point. The most complex criticality belongs to topology III, where the first-order line now divides the continuous critical line by two critical end points. In topology IV, the first-order line and the continuous line are met by a tricritical point. Accordingly, topology I presents one ferromagnetic phase, whereas the rest show two distinct ferromagnetic orders at low temperatures. On the other hand, the tricritical behavior manifested in topology IV emerges for $p > p^*$, where p^* denotes the probability for a given σ/J, where a fourth-order critical point is found. This point may be regarded as the last tricritical point vanishing for $\sigma/J > 0.202$, since $\sigma/J = 0.202$ leads to $p^* = 1$. Consequently, the tricritical behavior is no longer found for any p. Topology III disappears for $\sigma/J > 0.283$ and topology II is limited by $\sigma/J = 0.3989$, above which the first-order line separating the two ferromagnetic phases is suppressed for any p. After that, for $\sigma/J > 0.3989$, only the simplest topology survives.

Therefore, we show through this model how a complex magnetic criticality is reduced by the strength of the disorder (see also [28, 30, 31]). In finite dimensions, as far as we know, a few works related to the Blume–Capel model are found analyzing how above certain amount of [32, 33] (or by any amount of [7]) quenched randomness in the crystal field the multicritical behavior disappears. Nevertheless, the critical dimensions for these types of phase diagrams is still an open problem to be solved.

Acknowledgment

Financial support from CNPq (Brazilian agency) is acknowledged.

References

[1] Binder K and Young A P 1986 *Rev. Mod. Phys.* **58** 801
[2] Ghosal A, Randeria M and Trivedi N 1998 *Phys. Rev. Lett.* **81** 3940
[3] Belanger D P 1998 *Spin Glasses and Random Fields* ed A P Young (Singapore: World Scientific)
[4] Hui K and Berker A N 1989 *Phys. Rev. Lett.* **62** 2507
[5] Berker A N 1991 *J. Appl. Phys.* **70** 5941
[6] Aizenman M and Wehr J 1989 *Phys. Rev. Lett.* **62** 2503
[7] Branco N S and Boechat B M 1997 *Phys. Rev.* B **56** 11673
[8] Blume M 1966 *Phys. Rev.* **141** 517
[9] Capel H W 1966 *Physica (Utr.)* **32** 966
[10] Blume M, Emery V J and Griffiths R B 1971 *Phys. Rev.* A **4** 1071
[11] Mahan G D and Girvin S M 1978 *Phys. Rev.* B **17** 4411

[12] Jain jain K and Landau D P 1980 *Phys. Rev.* B **22** 445
[13] Grollau S, Kierlik E, Rosinberg M L and Tarjus G 2001 *Phys. Rev.* E **63** 041111
[14] Kutlu B, Ozkan A, Seferogu N, Solak A and Binal B 2005 *Int. J. Mod. Phys.* B **16** 933
[15] Seferoglu N, Ozkan A and Kutlu B 2006 *Chin. Phys. Lett.* **23** 2526
[16] Clusel M, Fortin J-Y and Plechko V N 2008 *J. Phys. A: Math. Theor.* **41** 405004
[17] Care C M 1993 *J. Phys. A: Math. Gen.* **26** 1481
[18] Beale P D 1985 *Phys. Rev.* B **33** 1717
[19] Silva C J and Caparica A A 2006 *Phys. Rev.* E **73** 036702
[20] Aharony A 1978 *Phys. Rev.* B **18** 3318
[21] Fytas N G, Malakis A and Eftaxias K 2008 *J. Stat. Mech.* P03015
[22] Ez-Zahraouy H and Kassou-Ou-Ali A 2004 *Phys. Rev.* B **69** 064415
[23] Benyoussef A, Biaz T, Saber M and Touzani M 1987 *J. Phys. C: Solid State Phys.* **20** 5349
[24] Carneiro C E I, Henriques V B and Salinas S R 1989 *J. Phys.: Condens. Matter* **1** 3687
[25] Carneiro C E I, Henriques V B and Salinas S R 1990 *J. Phys. A: Math. Gen.* **23** 3383
[26] Kaufman M and Kanner M 1990 *Phys. Rev.* B **42** 2378
[27] Kaufman M, Kluzinger P E and Khurana A 1986 *Phys. Rev.* B **34** 4766
[28] Salmon O R, Crokidakis N and Nobre F D 2009 *J. Phys.: Condens. Matter* **21** 056005
[29] Stanley H E 1971 *Introduction to Phase Transitions and Critical Phenomena* (Oxford: Clarendon)
[30] Crokidakis N and Nobre F D 2008 *Phys. Rev.* E **77** 041124
[31] Crokidakis N and Nobre F D 2008 *J. Phys.: Condens. Matter* **20** 145211
[32] Falikov A and Berker N 1996 *Phys. Rev. Lett.* **76** 4380
[33] Puha I and Diep H T 2001 *J. Magn. Magn. Mater.* **224** 85